JOC*Article*

Conformations and Threshold Rotational Mechanisms of C_5Ar_5 and C_5Ar_4X Molecular Propellers: A Structure Correlation and Computational Study

Stacey Brydges* and Michael J. McGlinchey*

Department of Chemistry, McMaster University, Hamilton, Ontario, Canada L8S 4M1

mcglinc@mcmaster.ca; brydges@mcmaster.ca

Received February 25, 2002

Crystallographically independent structures possessing persubstituted cyclopentadiene and -dienyl moieties were retrieved from the Cambridge Structural Database, and the torsional angles of selected diaryl frames presented in the form of conformational plots. Semiempirical calculations of the corresponding potential energy surfaces reproduced the conformational trends observed in the solid state. By the structure correlation principle, the internal oscillations of nearest (1,2-) and next-nearest (1,3-) aryl rings in all pseudopropeller subunits were found to be only partially correlated. These solid-state data sets, in combination with energetic predictions of the molecules $C_5Ph_5^-$ (**1**), $C_5Ph_4H^-$ (**2**), $C_4Ph_4C{=}O$ (**3**), and $C_4Ph_4CH_2$ (**4**) reveal that a *delayed n-ring-flip* (where $n = 4$ and 5 in $C_nAr_{n-m}X_m$), which is otherwise unobservable via NMR spectroscopic methods, is the threshold rotational mechanism.

Introduction

Among the numerous organic architectures presenting restricted conformational equilibria, molecular propellers have played a pivotal role in the development of modern stereochemical theory.[1] As a generic class of compounds composed of two or more substituents arranged in a helical fashion about either a central atom (type I)[2−9] or a planar, polyatomic framework (type II),[10−12] these constitutionally diverse, multiaryl systems are typically distinguished by their static and dynamic stereochemical attributes.[13] On the NMR timescale of observation, the former species generally exist in a chiral array (triphenylmethane, with its low enantiomerization barrier, is a notable exception[4a−f]), whereas derivatives of the latter type effectively possess an achiral, orthogonal perimeter. Analysis of torsional isomerism in appropriately substituted propeller units has revealed two seemingly disparate modes of rearrangements: correlated and uncorrelated ring rotation (Scheme 1). More specifically, helicity inversion in type I systems is achieved by means of "*n*-ring-flip" mechanisms that involve conrotatory rotation of *n* rings through a direction perpendicular to the

* Phone: (905)-525-9140 ext. 27699. Fax: (905)-522-2509.

(1) For reviews on molecular propellers, see: (a) Mislow, K.; Gust, D.; Finocchiaro, P.; Boettcher, R. J. *Fortschr. Chem. Forsch.* **1974**, *47*, 1−28. (b) Mislow, K. *Acc. Chem. Res.* **1976**, *9*, 26−33. (c) Meurer, K. P.; Vögtle, F. *Top. Curr. Chem.* **1985**, *127*, 3−75. (d) Willem, R.; Gielen, M.; Hoogzand, C.; Pepermans, H. *Advances in Dynamic Stereochemistry;* Gielen, M., Ed.; Academic Press: New York, 1985; Vol. 1, p 207.

(2) Diaryl-sulfoxides, -sulfones, -ethanols, and -ethers: (a) Casarani, D.; Grilli, S.; Lunazzi, L.; Mazzanti, A. *J. Org. Chem.* **2001**, *66*, 2757−2763. (b) Grilli, S.; Lunazzi, L.; Mazzanti, A. *J. Org. Chem.* **2001**, *66*, 5853−5858.

(3) Di- and triarylboranes: (a) Blount, J. F.; Finocchiaro, P.; Gust, D.; Mislow, K. *J. Am. Chem. Soc.* **1973**, *95*, 7019−7028. (b) Blount, J. F.; Finocchiaro, P.; Gust, D.; Mislow, K. *J. Am. Chem. Soc.* **1973**, *95*, 7029−7037.

(4) Triarylmethanes and triarylcarbenium ions: (a) Gust, D.; Mislow, K. *J. Am. Chem. Soc.* **1973**, *95*, 1535−1547. (b) Finocchiaro, P.; Gust, D.; Mislow, K. *J. Am. Chem. Soc.* **1974**, *96*, 2165−2167. (c) Andose, J. D.; Mislow, K. *J. Am. Chem. Soc.* **1974**, *96*, 2168−2176. (d) Finocchiaro, P.; Gust, D.; Mislow, K. *J. Am. Chem. Soc.* **1974**, *96*, 2176−2182. (e) Finocchiaro, P.; Gust, D.; Mislow, K. *J. Am. Chem. Soc.* **1974**, *96*, 3205−3213. (f) Levendis, D. C.; Bernal, I. *Struct. Chem.* **1997**, *8*, 263−273. (g) Ito, S.; Morita, N.; Asao, T. *Tetrahedron Lett.* **1992**, *44*, 6669−6672. (h) Ito, S.; Morita, N.; Asao, T. *Bull. Chem. Soc. Jpn.* **1995**, *68*, 1409−1436.

(5) Trialkoxymethanes: Willem, R.; Hoogzand, C. *Org. Magn. Reson.* **1979**, *12*, 55−58.

(6) Triarylamines: Glaser, R.; Blount, J. F.; Mislow, K. *J. Am. Chem. Soc.* **1980**, *102*, 2777−2786.

(7) Triarylphosphines and derivatives: (a) Howell, J. A. S.; Palin, M. G.; Yates, P. C.; McArdle, P.; Cunningham, D.; Goldschimdt, Z.; Gottlieb, H. E.; Hezroni-Langerman, D. *J. Chem. Soc., Perkin Trans. 2* **1992**, 1769−1775. (b) Howell, J. A. S.; Fey, N.; Lovatt, J. D.; Yates, P. C.; McArdle, P.; Cunningham, D.; Sadeh, E.; Gottlieb, H. E.; Goldschmidt, Z.; Hursthouse, M. B.; Light, M. E. *J. Chem. Soc., Dalton Trans.* **1999**, 3015−3028.

(8) Polyaryl-ethanes and -ethylenes: (a) Willem, R.; Pepermans, H.; Hallenga, K.; Gielen, M.; Dams, R. *J. Org. Chem.* **1983**, *48*, 1890−1898. (b) Rappoport, Z.; Biali, S. E. *Acc. Chem. Res.* **1997**, *30*, 307−314.

(9) Multiple-propeller units: (a) Lindner, A. B.; Grynszpan, F.; Biali, S. E. *J. Org. Chem.* **1993**, *58*, 6662−6670. (b) Selzer, T.; Rappoport, Z. *J. Org. Chem.* **1996**, *61*, 7326−7334. (c) Sedó, J.; Ventosa, N.; Molins, M. A.; Pons, M.; Rovira, C.; Veciana, J. *J. Org. Chem.* **2001**, *66*, 1567−1578. (d) Sedó, J.; Ventosa, N.; Molins, M. A.; Pons, M.; Rovira, C.; Veciana, J. *J. Org. Chem.* **2001**, *66*, 1579−1589.

(10) Tetraarylcyclopentadienones: (a) Willem, R.; Pepermans, H.; Hoogzand, C.; Hallenga, K.; Gielen, M. *J. Am. Chem. Soc.* **1981**, *103*, 2299−2306. (b) Willem, R.; Jans, A.; Hoogzand, C.; Gielen, M.; Van Binst, G.; Pepermans, H. *J. Am. Chem. Soc.* **1985**, *107*, 28−32.

(11) Pentaarylpyrroles: Fagan, M. W.; Gust, D. *J. Org. Chem.* **1981**, *46*, 1499−1500.

(12) Hexaarylbenzenes: (a) Gust, D. *J. Am. Chem. Soc.* **1977**, *99*, 6980−6982. (b) Gust, D.; Patton, A. *J. Am. Chem. Soc.* **1978**, *100*, 8175−8181. (c) Patton, A.; Dirks, J. W.; Gust, D. *J. Org. Chem.* **1979**, *44*, 4749−4752. (d) Pepermans, H.; Willem, R.; Gielen, M.; Hoogzand, C. *J. Org. Chem.* **1986**, *51*, 301−306.

(13) The propeller classification scheme used here is not rigid (other criteria, such as C_n or D_n symmetry, may be invoked) but is implemented for the purpose of the stereochemical arguments advanced by Pepermans and co-workers.

10.1021/jo0201272 CCC: $22.00
Published on Web 10/08/2002

SCHEME 1. Stereoisomerization in (a) Triarylmethanes and (b) Hexaarylbenzenes, Two Classic Examples of Molecular Propellers[a]

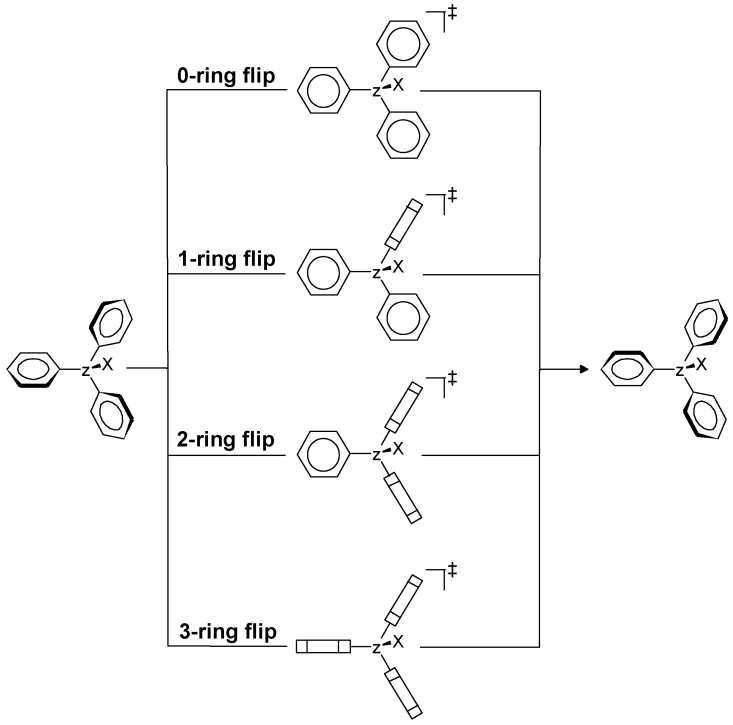

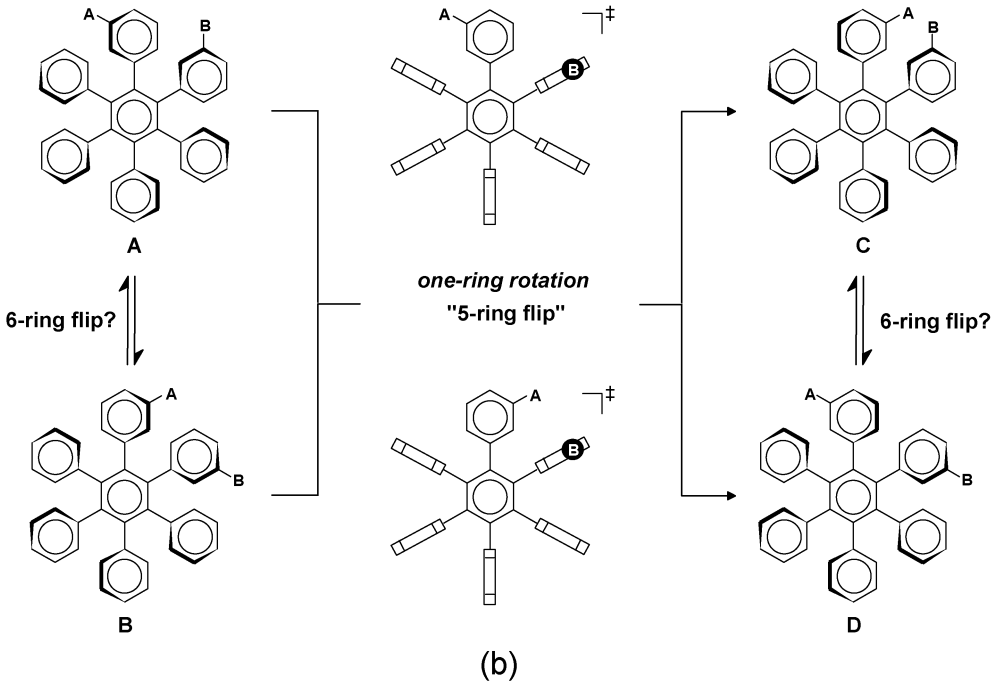

[a] Stereoisomerization is conventionally distinguished by correlated ("*n*-ring flip") and uncorrelated (180° edge-interchange of an individual ring) rotational pathways. Since helicity inversion is only inferred in the latter case, syn-anti interconversion may theoretically occur by two diverse mechanisms: 180°-one-ring rotation (A → C; B → D) or a five-ring flip (A → D; B → C)

propeller plane, while the nonflipping rings, if any, pass (relative to the *n* rings) in a disrotatory fashion through the reference plane, with concomitant edge interchange. This sympathetic motion is the basis for an intriguing phenomenon, residual stereoisomerism,[1b,14] and has evoked analogies to macroscopic bevel gears (the "cog-wheel effect").[15,16] For type II molecules, the topomerization pathway (i.e., process of site exchange) of lowest energy consists of the independent rotation of a single peripheral

(14) Finocchiaro, P.; Gust, D.; Mislow, K. *J. Am. Chem. Soc.* **1974**, *96*, 3198−3205.

ring by 180° and proceeds with indeterminate helicity (at least by NMR spectroscopy). However, Willem, Pepermans et al.[8a] have reasoned that the two models are equivalent from a permutational perspective, since the one-ring rotation of the perpendicular conformation and the $(n-1)$-ring flip of the propeller forms are stereochemically correspondent.[1a] In accordance with this unified classification scheme, the threshold mode of isomerization of *all n*-aryl propeller systems is either a (n) or $(n-x$, where $x \leq m)$-ring flip.

Such a dynamic analogy implies that the effective NMR time-averaged perpendicular conformation of C_nAr_n and $C_nAr_{n-m}X_m$ propeller systems represents an idealized transition state for the low-energy interconversion of helical forms via a concerted *n*-ring flip. Notwithstanding the intuitive logic of this rotational phenomenon, incompatible timescale considerations have precluded its experimental verification. To circumvent this issue, previous analyses of torsional behaviors of particular di- and triaryl systems, including 1,1- and 1,2-diarylethenes,[17,18] benzophenones,[19] and triphenylphosphine oxides,[20] have employed the structure correlation (SC) method.[21,22]

The statistical survey of solid-state structural data requires an examination of the perturbation of a given fragment geometry within different intra- and intermolecular environments (steric setting, crystal packing arrangements), allowing for a series of crystallographic "snapshots" of the process under investigation. In the low-energy regions of *n*-dimensional space there should be a concentration of sample points corresponding to the favored conformation; as the energy rises, the reaction path becomes increasingly less populated in the vicinity of the associated transition state. As stated by Bürgi and Dunitz, "If a correlation can be found between two or more independent parameters describing the structure of a given molecular fragment in various environments, then the correlation function maps a minimum energy path in the corresponding parameter space."[21] Accordingly, a succession of static X-ray structures of C_5Ar_5 and C_5Ar_4X derivatives should permit us to survey the potential energy surface associated with interannular rotations and therefore improve our understanding of the stereoisomerization processes exhibited by these propeller systems. To date, their fluxional properties have been interpreted using the stereochemical framework proposed for hexaarylbenzenes (vide supra). However, the SC method is particularly relevant for low barrier rotational pathways for which the slow exchange NMR regime cannot be accessed experimentally. As a supplement to the activation parameters that have been acquired by use of dynamic NMR, we present herein a study of the conformational preferences and associated threshold rotational pathways of persubstituted cyclopentadiene and -dienyl moieties by application of structure correlation principles.

Experimental Section

Conformational Maps and Computational Methods. The torsional preferences and variability of C_5Ar_5 and C_5Ar_4X molecules can be conveniently analyzed by means of a conformational map[23] (cf. also a Ramachandran-type plot[24]), which depicts the relative energy as a function of the central-to-peripheral ring interplanar angles (ϕ_n) of interest. The symmetry properties of the two-dimensional rotational potential energy surface reflect the symmetry of the nonrigid molecular fragment, which is isometric to either C_{2v} {[1,2-], [1,3-] (C_5Ar_5); [2,3-], [1,4-] (C_5Ar_4X)} or C_s {[1,2-], [1,3-] (C_5Ar_4X)} for the idealized diaryl frames. The relative energies of $C_5Ph_5^-$ (**1**), $C_5Ph_4H^-$ (**2**), $C_4Ph_4C{=}O$ (**3**), and $C_4Ph_4CH_2$ (**4**) were calculated at the semiempirical level of theory (AM1 Hamiltonian)[25] by systematically altering the two selected angles ϕ_n in 10° increments (dihedral driver option in SPARTAN V5.1[26]) from 0° to 90° and 0° to 180°, while allowing all other torsional degrees of freedom to minimize accordingly. For comparative purposes, the conformational plots were also generated using molecular mechanics methods (MMFF94[27] and Sybyl[28] force fields) and have been provided as Supporting Information. To confirm the nature of specific stationary points along the PES of **1**−**4** (Table 1), geometry optimizations and subsequent frequency analyses were performed using the AM1 Hamiltonian as implemented in the GAUSSIAN98 program suite.[29] The visualization and depiction of structures was enabled with QMView.[30]

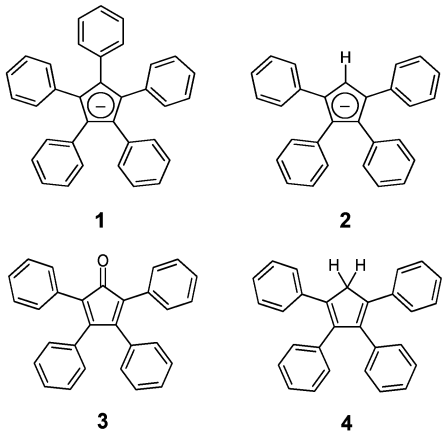

1 **2** **3** **4**

Database Retrieval. A Cambridge Structural Database (July 2001 version)[31] search was conducted of molecular fragments possessing C_5Ar_4X ($X \neq Ar$) and C_5Ar_5 formulations, and incorporated those with peripheral aryl substitution, metal coordination, charged species, and geometrically nonconstrained (i.e., nonfused aromatics) frameworks. For the initial study, cyclopentadienyl species displaying a deviation from planarity of the central C_5-ring >0.05 Å and a crystallographic agreement *R* factor >0.10 were excluded; no further restrictions were placed on the nonbonding interactions (packing phenomena).

Data Treatment. Atomic coordinates of 62 crystallographically independent substructures derived from 48 C_5Ar_5 units

(15) Iwamura, H.; Mislow, K. *Acc. Chem. Res.* **1988**, *21*, 175−182.
(16) Hounshell, W. D.; Iroff, L. D.; Iverson, D. J.; Wroczynski, R. J.; Mislow, K. *Isr. J. Chem.* **1980**, *20*, 65−71.
(17) Kaftory, M.; Nugiel, D. A.; Biali, S. E.; Rappoport, Z. *J. Am. Chem. Soc.* **1989**, *111*, 8181−8191.
(18) Gur, E.; Kaftory, M.; Biali, S. E.; Rappoport, Z. *J. Org. Chem.* **1999**, *64*, 4, 8144−8148.
(19) Rappoport, Z.; Biali, S. E.; Kaftory, M. *J. Am. Chem. Soc.* **1990**, *112*, 7742−7748.
(20) Bye, E.; Schweizer, W. B.; Dunitz, J. D. *J. Am. Chem. Soc.* **1982**, *104*, 5893−5898.
(21) Bürgi, H.-B.; Dunitz, J. D. *Acc. Chem. Res.* **1983**, *16*, 153−161.
(22) Bürgi, H. B.; Dunitz, J. D. *Structure Correlation*; VCH: Weinheim, New York, 1994.
(23) Dunitz, J. D. *X-ray Analysis and the Structure of Organic Molecules*; Cornell University Press: Ithaca, NY, 1979; Chapter 10.
(24) Ramachandran, G. N.; Sasisekharan, V. *Adv. Protein Chem.* **1968**, *23*, 283−438.
(25) Dewar, M. J. S.; Zoebisch, E. G.; Healy, E. F.; Stewart, J. J. P. *J. Am. Chem. Soc.* **1985**, *107*, 3902−3909.
(26) SPARTAN SGI Version 5.1.1, Wavefunction, Inc.: Irvine, CA.
(27) Halgren, T. A. *J. Comput. Chem.* **1996**, *17*, 490−519.
(28) Clark, M.; Cramer, R. D., III; Van Opdenbosch, N. *J. Comput. Chem.* **1989**, *10*, 982−1012.

TABLE 1. Calculated (AM1) Conformational Energies of Molecules 1−4

	interconversion process[a]	E (au)	ΔE (kcal mol^{-1})[b]	Ph-C_5 ∠ (deg)
1-D_5		0.213809	0.0*	46.3
1-D_{5h}	5-ring flip	0.205231	5.4	90.0
1-C_{2v}	4-ring flip	0.214266	5.7	90.0, 0.0
1-TS1	sequential-5-ring flip	0.207888	1.7**	109.4, 75.2 (α), 40.5 (*β*)
2-C_2		0.161710	0.0*	30.3 (α), 47.1 (*β*)
2-C_s		0.162971	0.8**	25.1 (α), 72.6 (*β*)
2-C_{2v}	4-ring flip	0.174078	7.8	90.0
2-C_s	[α,*β*,*β*]-3-ring flip	0.169106	4.6	90.0, 0.0 (α)
2-C_s'	[α,α,*β*]-3-ring flip	0.173318	7.3	90.0, 0.0 (*β*)
2-TS1	sequential-4-ring flip	0.165666	2.5**	110.0 (α), 51.0, 41.9 (*β*), 31.5 (α)
3-C_2		0.198769	0.0*	30.4 (α), 76.9 (*β*)
3-C_s		0.198916	0.1*	30.8 (α), 81.0 (*β*)
3-C_{2v}	4-ring flip	0.204465	3.6	90.0
3-C_s	[α,*β*,*β*]-3-ring flip	0.203215	2.8	90.0, 0.0 (α)
3-C_s'	[α,α,*β*]-3-ring flip	0.209080	6.5	90.0, 0.0 (*β*)
3-TS1	sequential-4-ring flip	0.201328	1.6**	110.3 (α), 73.9, 77.0 (*β*), 31.4 (α)
4-C_2		0.222599	0.0*	30.3 (α), 79.3 (*β*)
4-C_s		0.222696	0.1*	30.0 (α), 81.5 (*β*)
4-C_{2v}	4-ring flip	0.226683	2.6	90.0
4-C_s	[α,*β*,*β*]-3-ring flip	0.225049	1.5	90.0, 0.0 (α)
4-C_s'	[α,α,*β*]-3-ring flip	0.231271	5.4	90.0, 0.0 (*β*)
4-TS1	sequential-4-ring flip	0.224236	1.0**	106.4 (α), 60.3, 80.4 (*β*), 30.4 (α)

[a] Abbreviated titles are used here (see text). [b] Second derivative analyses have confirmed that these stationary points are either a local (*) minimum or a (**) transition state; otherwise, the structures represent higher *n*th-order saddle points (*n* negative eigenvalues).

were retrieved using the CSD programs QUEST and CONQUEST (see Supporting Information tables). Likewise, data for 100 substructures were acquired from 86 C_5Ar_4X units (where X ≠ Ar). The C_5Ar_4X subset was further divided into two structural classes, comprising either aromatic (cyclopentadienyl) or nonaromatic (cyclopentadiene) systems. The torsional angles (defined as the angle between the mean planes of the peripheral ring and internal C_5-ring (C_5Ar_5 or C_5Ar_4X) or diene fragment (C_5Ar_4X), and denoted as ϕ_1, ϕ_2, ϕ_3, ϕ_4, ϕ_5, where the X substituent is always designated at position 5 for consistency) were analyzed manually, selecting as the reference frame the *z*-axis as directed along the ML_n-central Cp bond.[32] To eliminate the arbitrariness inherent in labeling the directionality of the interplanar angles, isometric conformations have been included.[33] A comparison of several molecular fragments requires each specimen to be considered as a representative point (terminus of vector) in an *n*-dimensional hyperspace, with one dimension for each internal coordinate of interest. The simultaneous analysis of the five or four peripheral rings in C_5Ar_5 and C_5Ar_4X structures would therefore necessitate a 5th (4th) dimensional mathematical (principal component or cluster analysis) treatment and presentation (hyperstereoscopic unit cell, for example) of the data. Obviously there is a practical limitation to this approach, given the difficulties associated with visualization and, hence, interpretation of the results. In reducing the problem to two- or three-dimensional parameter space, the chemical questions that may be addressed by such a study are significantly modified. Rather than portraying the interdependence of all aryl substituents, a two-dimensional correlation of torsional angles of nearest (or next-nearest) neighbors (cf. histogram or conformational map) highlights the conformational relationship of such fragments exclusively. The latter graphical method requires that each C_5Ar_5 or C_5Ar_4X moiety contribute not one, but five or four data points, respectively, exclusive of its isometric conformations. Whereas this precludes the direct investigation of a threshold rotational mechanism in these systems, it provides insight into contiguous group effects and the preferred arrangement of such molecules. *As the torsional angle of a peripheral aryl ring-to-central plane changes, what influence, if any, does this have on neighboring aryl groups? Does the variation in molecular geometry provide any evidence of gearing motion or correlated rotation in these systems?*

Results and Discussion

Histogram Analysis. The histograms depicted in Figure 1 were generated from the absolute values of peripheral aryl-to-central ring interplanar angles for the collective crystallographic sets of C_5Ar_5 and C_5Ar_4X molecules. A comparison of the distribution of angles reveals comparable medians (cf. 51.1° (C_5Ar_5), 50.1° (dienyl), and 51.0° (diene), respectively), whereas the range of values is much greater in the latter systems (cf. 77.5° (dienyl), 73.6° (diene), and 61.6°(C_5Ar_5)). Moreover, the relatively peaked distribution (kurtosis[34] = 1.97) displayed by the C_5Ar_5 systems is in contrast to the more uniform dispersion (kurtosis = −0.70 for dienyl species

(29) Frisch, M. J.; Trucks, G. W.; Schlegel, H. B.; Scuseria, G. E.; Robb, M. A.; Cheeseman, J. R.; Zakrzewski, V. G.; Montgomery, Jr., J. A.; Stratmann, R. E.; Burant, J. C.; Dapprich, S.; Millam, J. M.; Daniels, A. D.; Kudin, K. N.; Strain, M. C.; Farkas, O.; Tomasi, J.; Barone, V.; Cossi, M.; Cammi, R.; Mennucci, V.; Pomelli, C.; Adamo, C.; Clifford, S.; Ochterski, J.; Petersson, G. A.; Ayala, P. Y.; Cui, Q.; Morokuma, K.; Malick, D. K.; Rabuck, A. D.; Raghavachari, K.; Foresman, J. B.; Cioslowski, J.; Ortiz, J. V.; Baboul, A. G.; Stefanov, B. B.; Liu, G.; Liashenko, A.; Piskorz, P.; Komaromi, V.; Gomperts, R.; Martin, R. L.; Fox, D. J.; Keith, T.; Al-Laham, M. A.; Peng, C. Y.; Nanayakkara, A.; Challacombe, M.; Gill, P. M. W.; Johnson, B.; Chen, W.; Wong, M. W.; Andres, J. L.; Gonzalez, C.; Head-Gordon, M.; Replogle, E. S.; Pople, J. A. *GAUSSIAN 98*, Rev. A.9; Gaussian: Pittsburgh, PA, 1998.

(30) Baldridge, K. K.; Greenberg, J. P. *J. Mol. Graphics* **1995**, *13*, 63.

(31) *CSD*, July Release V5.21 2001; Cambridge Crystallographic Data Center: University Chemical Laboratory, Cambridge, England.

(32) For such purposes, the torsional angles were appropriately adjusted to be less than 90° (where 90° corresponds to the orthogonal conformation of a peripheral ring to the central plane) while still maintaining their sign. Published coordinates refer to an arbitrarily chosen sense of chirality; (180° − dihedral angle) generates the enantiomeric structure.

(33) The symmetry operations of the molecular frame convert a given conformation (or representative point, p(ϕi,ϕj)) into a set of equivalent, isometric conformations (or points).

(34) *Kurtosis* = $(\Sigma(X - \mu)^4/N\sigma^4) - 3$ where μ is the mean, σ is the standard deviation, and N is the number of data points. Kurtosis is based on the size of a distribution's tails, with values corresponding to a high peak (> 0), a flat-topped curve (< 0), or a normal distribution (= 0).

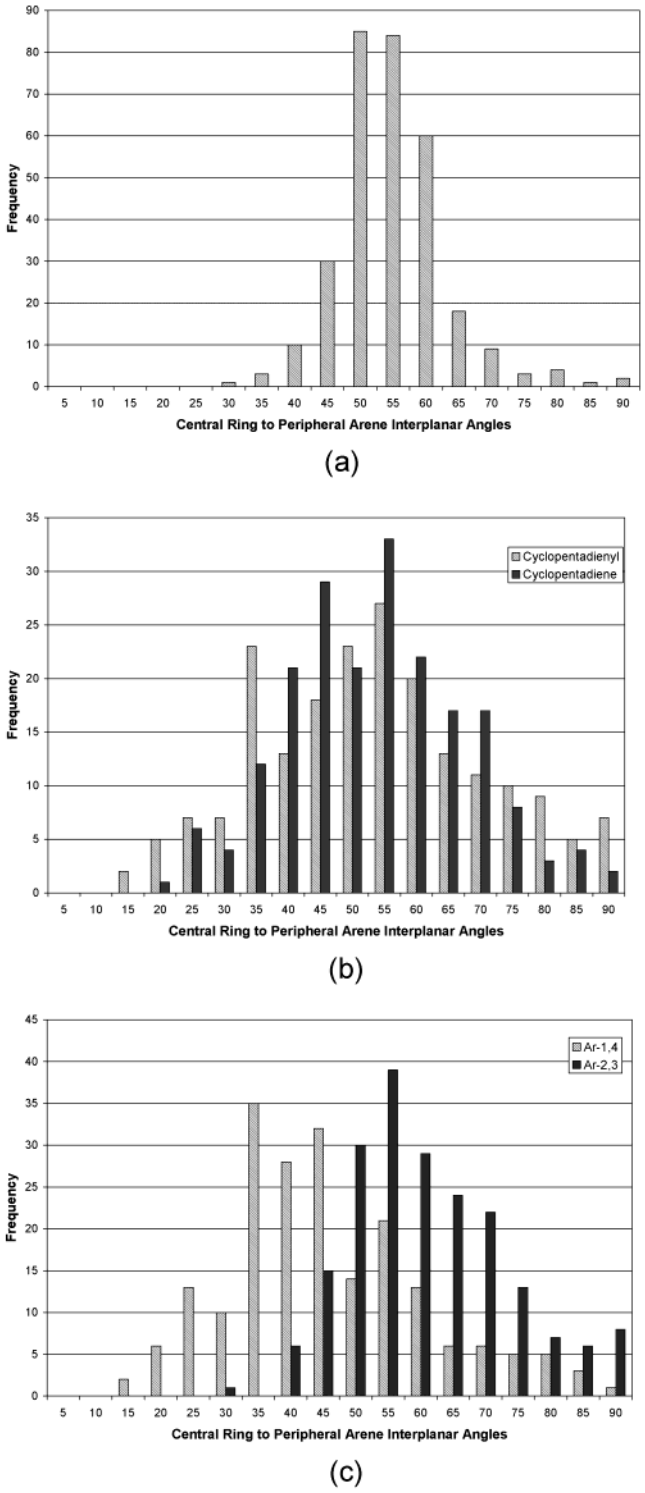

FIGURE 1. Distribution of interplanar angles (with bin sizes of 5° increments) for all aryl substituents in (a) C_5Ar_5 and (b) C_5Ar_4X systems, with α (1,4) and β (2,3) aryl groups also depicted separately in (c) for the latter case.

and −0.78 for diene fragments) that characterizes the C_5Ar_4X fragments. If the entire series of C_5Ar_4X interplanar angles is partitioned into two subsets comprising aryl groups positioned α (1,4) and β (2,3) to the X substituent, a significantly different distribution is apparent (Figure 1c). 1,4-Interplanar angles are scattered over a range of 75.6°, with a median of 40.5° and associated kurtosis of 0.19. Centered at 56.7°, the 2,3-interplanar angles envelop a smaller region (60.2°) with a kurtosis (−0.30) reflective of the skew toward an orthogonal orientation. These trends confirm our simple chemical intuition that aryl-flanked β rings are more sterically encumbered than α rings (i.e., when X is less bulky than an aryl group), which exhibit a heightened rotational response to intra- and intermolecular nonbonded interactions.

C_5Ar_5 Systems. In all pentaarylcyclopentadienyl systems thus far examined by use of dynamic NMR, independent peripheral ring rotation by $\sim\pi$ radians has been invoked as the stereoisomerization mechanism of lowest observable energy.[35] However, a small phenyl group oscillation about the planes orthogonal to the C_5 ring of the neutral C_5Ph_5 radical has been deduced from EPR spectroscopy.[36] Furthermore, the splitting of the solution C−O stretching absorptions in the solid-state IR spectra of several chiral complexes, including [Fe(η^5-C_5Ph_5)(CO)(PMe$_3$)Br] (**5**),[37] [Os(η^5-C_5Ph_5)(CO)(L)Br] where L = PMe$_2$Ph (**6**), P(OEt)$_3$ (**7**), and P(OCH$_2$)$_3$CCH$_3$ (**8**),[38] has been rationalized on the basis of diastereoisomerism, arising from the propeller helicity.

The symmetry-extended conformations of C_5Ar_5 fragments possessing two internal rotational degrees of freedom are mapped in Figure 2. With the exception of values corresponding to three moieties,[39] the solid-state data points (Table S.1, Supporting Information) lie in the region where both torsional angles have the same sign, which is the condition for a propeller structure. This arrangement is typically favored as a result of a compromise between energy-reducing conjugation effects (maximal when the peripheral aryl substituents are coplanar with the central ring) and energy-increasing repulsive steric effects (minimal when the aryl groups are perpendicular to the C_5 ring). From the pronounced clustering of points around (∼50°, ∼50°), sparsely populated symmetry-related paths corresponding to torsional angles of opposite sign {via regions (∼90°, ∼50°) to (∼130°, ∼50°)} interconnect enantiomeric conformations (e.g., (50°, 50°) and (−50°, −50°) = (130°, 130°)). The same trend is exhibited by both adjacent (1,2-) and next-nearest (1,3-) aryl groups (Figure 2a and b, respectively), although there is a wider data spread in the latter case. As a plausible description of the stereomutation process that is manifested here, uncorrelated rotation can be discounted since minima of identical helicities are segregated. Furthermore, the absence of points near the (∼90°, ∼90°), (∼0°, ∼90°), and (∼90°, ∼0°) regions suggests that helicity inversion of the propeller molecule is distinguished by neither a classical (concomitant) conrotatory nor a disrotatory pathway. Instead the data, which encapsulate all C_5Ar_5 interplanar angles, are more readily interpreted in terms of a delayed 5-fold motion;

(35) For a summary and discussion, see: Brydges, S.; Harrington, L. E.; McGlinchey, M. J. *Coord. Chem. Rev.* **2002**, in press, and references therein.

(36) Möbius, K. *Z. Naturforsch.* **1965**, *20A*, 1117−1121.

(37) Brégaint, P.; Hamon, J.-R.; Lapinte, C. *Organometallics* **1992**, *11*, 1417−1419.

(38) Field, L. D.; Hambley, T. W.; Humphrey, P. A.; Masters, A. F.; Turner, P. *Polyhedron* **1998**, *17*, 2587−2598.

(39) While there are no obvious steric interactions that may explain the helical distortions in two of the organometallic derivatives (HOGPAU, SIRMIP), in the third case (HAYMEZ) it is the presence of a palladium-bound 2,6-dimethylphenylisocyanido ring wedged between two contiguous peripheral phenyl groups that appears to engender the nonpropeller C_5Ph_5 array in one of its crystallographic forms.

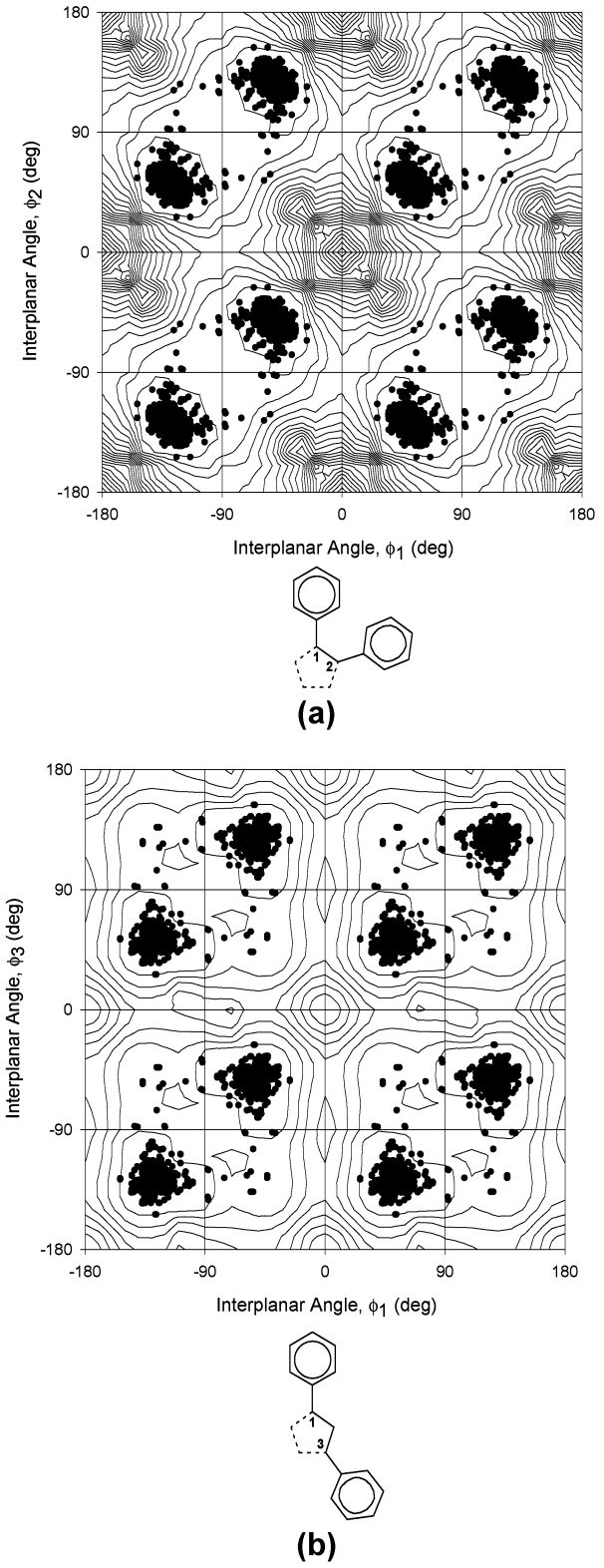

FIGURE 2. Conformational maps of torsional angles of two peripheral aryl rings (or rotors) constituting part of a C_5Ar_5 frame, featuring (a) adjacent (1,2) aryl groups, and (b) next-nearest neighboring (1,3) aryl groups. In both maps a denser population of points can be observed in the region of (~50°, ~50°), corresponding to the low-energy conformation of pentaarylcyclopentadienyl species. The overlayed contours (at 1 kcal mol^{-1}) represent the calculated (AM1) equipotential energy regions associated with $C_5Ph_5^-$ (**1**).

at a critical torsional angle, which likely coincides with the van der Waals distance, an instantaneous (conrotatory) ring flip occurs. Accordingly, this analysis provides the first evidence for a *nonclassical n*-ring ($n = 5$) flip interconversion process operative in these types of propeller systems.

The dynamic behavior of more complex C_5Ar_5 fragments may be qualitatively interpreted from the calculated potential energy surfaces of $C_5Ph_5^-$ **1**, in view of the correspondence between the contour maps and the preferred solid-state geometry of the molecules comprising the diversely substituted C_5Ar_5 subset. The PES regions of lowest ($\phi_1 = \phi_2 = 50 \pm 10°$; $\phi_1 = \phi_3 = 50 \pm 10°$) and highest ($\phi_1 = \phi_2 < 40°$; $\phi_1 = \phi_3 < 40°$) energy are consistent with the concentrated and uninhabited areas of the crystallographic scatterplots, respectively. The barriers to enantiomerization (helicity inversion) of the selected frames (1,2-Ar_2 and 1,3-Ar_2) may be estimated as 2−3 kcal mol^{-1} from the plots. In extrapolating the mechanistic information to the entire molecule, a more precise assessment of the energetics of this process requires characterization of the actual saddle point(s) separating the ground-state propellers of **1** (vide infra).

C_5Ar_4X Systems (Aromatic). Tetraarylcyclopentadienyl derivatives bearing X substituents also display restricted rotation on the NMR timescale. However, analogous to polyarylbenzenes,[12c] steric buttressing effects can influence the isomerization pathway and associated barrier heights. For example, in the ^{1}H VT-NMR spectra (293−183 K) of the ansa-metallocene complex, rac-[1-(η^5-Cp)-1-Ph-(η^5-C_5Ph_4)Et]$ZrCl_2$ **9**, the slowed rotation of the β phenyl groups (273 K) was detected in advance of the sterically less hindered α phenyls (253 K).[40] In the static ^{1}H VT-NMR limit (178 K) of the linear metallocene, $Fe(C_5Ph_4H)_2$ **10**, the high-frequency shift of the Cp proton has been attributed to deshielding from ring currents of the adjacent α rings, which are purported to assume a coplanar orientation relative to the central C_5 ring.[41] If qualitative parallels are drawn, peripheral substitution of the C_5 framework might also be expected to alter the conformational model for helicity inversion.

Semiempirical calculations of the tetraphenylcyclopentadienyl ligand (**2**) indicate that the molecule adopts a propeller orientation of C_2 symmetry, with interplanar angles of 30° (α) and 47° (β). As a conformational option, the C_s rotamer (ϕ_α ~25° and ϕ_β ~73°) is only 0.8 kcal mol^{-1} higher in energy than the global minimum and is associated with one imaginary vibrational frequency. When the various skeletal fragments are considered separately, the projected activation energies of this process are in the range of 2−3 kcal mol^{-1}.

The C_5Ar_4X (X ≠ Ar) subset is comprised of 50 data points (Table S.2, Supporting Information), wherein 26 fragments assume a propeller conformation, 9 adopt a nonpropeller arrangement (with only one aryl substituent canted in the opposite direction), and 15 possess a pseudomirror structure (with aryl groups 1 and 2 oppositely inclined to aryl rings 3 and 4). In comparison to C_5Ar_5 systems, the structural deformations within this

(40) Harrison, W. M.; Saadeh, C.; Colbran, S. B.; Craig, D. C. *J. Chem. Soc., Dalton Trans.* **1997**, 3785−3792.
(41) Castellani, M. P.; Wright, J. M.; Geib, S. J.; Rheingold, A. L.; Trogler, W. C. *Organometallics* **1986**, *5*, 1116−1122.

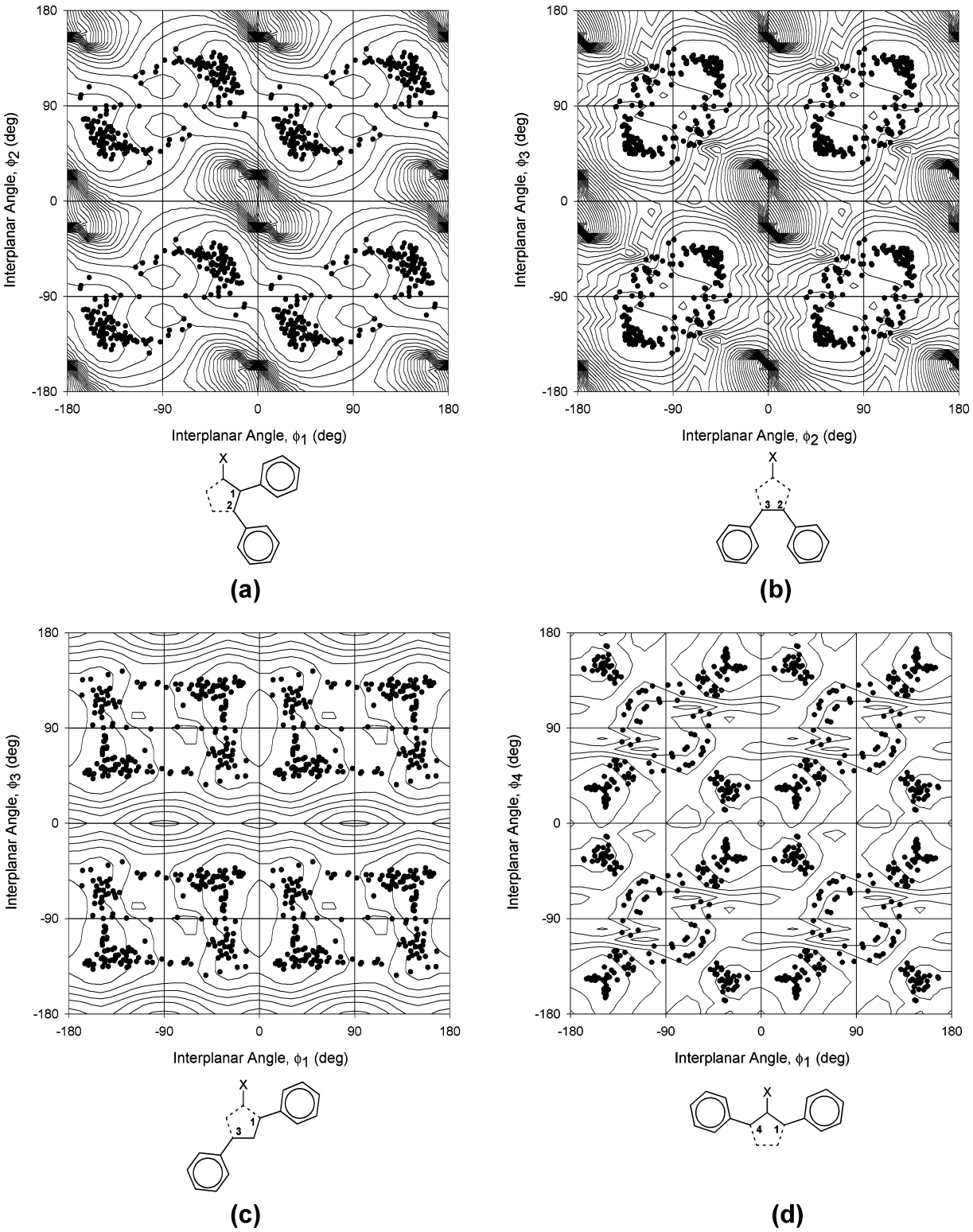

FIGURE 3. Conformational maps of torsional angles of two peripheral aryl rings (or rotors) constituting part of a C_5Ar_4X (X ≠ Ar) frame, featuring vicinal (a) (1,2/4,3) and (b) (2,3), as well as next-nearest (c) (1,3) and (d) (1,4) interactions. The overlayed contours (at 1.5 kcal mol^{-1}) represent the calculated (AM1) equipotential energy regions associated with $C_5Ph_4H^-$ (**2**).

class are more pronounced, attributable in part to the two sets of aryl groups (α and *β* to the X substituent) residing in differing steric environments. The sampling of C_5Ar_4X moieties therefore provides increased conformational coverage and the potential for further probing the stereodynamic details of these multirotor arrays.

The crystallographic data points for all C_5Ar_4X fragments are superimposed on the AM1 calculated PES for $C_5Ph_4H^-$ (**2**) in Figure 3, which depicts diaryl [1,2-/4,3-], [2,3-], [1,3-], and [1,4-] frameworks. For the symmetry inequivalent 1,2/4,3 model, most of the points congregate in the vicinity of (∼40°, ∼60°), and represent both

propeller and pseudomirror structures. The path linking equilibrium conformations is formed by nonpropeller fragments and proceeds via (∼120°, ∼75°), suggesting that α ring libration induces the *β* ring to flip. Although energetically accessible according to calculations, the (90°, 90°) region is void of data. Interestingly, three nonpropeller moieties yield rotational values that approach (0°, 90°), the *idealized* transition state for either an independent α-one-ring rotation[42,43] or a correlated α,*β*,*β*-3-ring flip.

In considering the 2,3-vicinal aryl substituents (Figure 3b), propeller and nonpropeller moieties both give rise to the enantiomeric clusters at (∼60°, ∼60°) and (∼120°, ∼120°), which are interconnected by symmetry-related pathways {via regions (∼90°, ∼60°) to (∼120°, ∼90°)} densely populated by pseudomirror structures. Once again, the progressive rotation of one ring through the orthogonal position gradually effects the helicity reversal of the adjacent ring. The asymmetry of this torsional circuit should not be overlooked; whereas α aryl substituents must traverse at least 100° to achieve enantiomerization, the rotational span of *β* aryl groups is only ∼60°.

The transformation of 1,3-diaryl enantiomeric conformations {(∼40°, ∼60°) to (∼140°, ∼120°), and (∼40°, ∼120°) to (∼140°, ∼60°)} proceeds via linear routes corresponding to a sequential 2-ring flip, wherein the inversion of the second aryl group appears instantaneous (Figure 3c). Extending the torsional scope to the least sterically encumbered (when X is less bulky than an aryl group) 1,4-diaryl interactions, the associated conformational map (Figure 3d) depicts separate enantiomeric clusters of propellers {(∼40°, ∼40°), (∼140°, ∼140°)} and pseudomirror structures {(∼40°, ∼140°), (∼140°, ∼40°)}, linked by nonpropeller fragments along a (90°, ∼60°); (∼120°, 90°) curvature.

The picture that emerges when all sets of torsional data are amassed suggests that helicity inversion in tetraarylated cyclopentadienyl systems is achieved by means of a *delayed* oscillation. Despite the fact that α and *β* aryl groups experience different buttressing effects, both immediate and long-range correlations may be ascribed to a lowest energy stereoisomerization pathway that is equivalent to a *nonsynchronous* 4-ring flip, in agreement with calculations. The flatness of the PE landscape near the dominant propeller conformation easily lends to deformations, with pseudomirror fragments corresponding to an energy transition, as predicted computationally.

C_5Ar_4X Systems (Non-Aromatic). The stereochemical scaffold for all substituted tetrahapto and pentahapto C_5Ar_4X ligands was derived from the detailed conformational analysis of tetraphenylcyclopentadienone (**3**). By analogy with C_6Ar_6 propellers, Willem, Pepermans, et al.[10a] proposed a static, C_{2v} symmetric $Ph_4C_4C{=}O$ skeleton in which the four aryl groups are orthogonal to the central C_5-ring, at least on the NMR timescale (see Scheme 1b). The VT-NMR spectral data of the maximally labeled tetra-*o*-tolylcyclopentadienone **11** were ascribed to two dynamic processes: a low energy, uncorrelated α-one-ring rotation (cf. α,*β*,*β*-3-ring flip) in the direction of the carbonyl moiety, and a more sterically demanding, uncorrelated *β*-one-ring rotation ($\Delta G^{\ddagger} \approx 20$ kcal mol^{-1}; cf. α,α,*β*-3-ring flip). As conceded by the authors, a model that embraces the interconversion of propeller configurations lends itself to the same combination of rearrangement modes and experimental rationales, provided the threshold rotational pathway is a concerted four-ring flip *or approximation thereof*. In probing this inversion process from a SC vantage, Hückel 4*n* systems present not only disparate steric influences of an X substituent relative to an aryl moiety, but additional electronic differences (and accompanying variations in bond lengths, bond angles, central ring deformability and central-to-peripheral ring conjugative effects) that may have stereochemical consequences.

The tetraarylcyclopentadiene solid-state subset is also composed of 50 data points (Table S.3, Supporting Information), with a conformational partitioning of 29 propeller, 5 nonpropeller, and 16 pseudomirror fragments. With reference to the hybridization of the C(5) center, both sp^2 (22) and sp^3 (28) derivatives have been included in this structural class. Statistically, more than half the $Ar_4C_4C{=}X$ moieties are cup-shaped, whereas almost 70% of the $Ar_4C_4CX_2$ units assume a helical arrangement.

AM1 calculations of tetraphenylcyclopentadienone (**3**) predict a chiral C_2 isomer with angles of ∼30° and 77° (cf. values of 27.4°, 60.5°, 47.7°, and 36.1° in the experimentally observed propeller[44]), as well as an almost equally accessible C_s-symmetric structure (ϕ_α ∼30° and ϕ_β ∼81°). These two conformations are essentially isoenergetic in tetraphenylcyclopentadiene (**4**), which adopts a pseudomirror structure with interplanar angles of 33.1°, 69.4°, 69.6°, and 23.5° in the solid state.[45]

Figure 4 features the experimental solid-state torsional values superimposed on the calculated PES of **3** for the various diaryl frames. Patterns similar to the C_5Ar_4X subset are manifested in all four plots; however, the data are generally more scattered, and the pathways connecting enantiomeric clusters are much less clearly defined. A survey of vicinal interactions (1,2/4,3 and 2,3) reveals that certain $Ar_4C_4CX_2$ structures contribute isometric angles which approach the (90°, 90°) region. Overall, the rotational trajectory is less evident from this data set, making it unreasonable to speculate about any stereochemical variations between the constitutionally distinct $Ar_4C_4C{=}X/Ar_4C_4CX_2$ and C_5Ar_5 ligands.

Threshold Rotational Mechanism. Having arranged the pillars of a dynamic model from the conformational energy landscapes of **1**−**4**, a more rigorous analysis of the degenerate inversions is now feasible. In the **1**-D_5 ⇌ **1**-D_5' isomerization, three transition states and two intermediates, differing in energy by less than 0.7 kcal mol^{-1}, have been identified (Scheme 2a). Scheme 3a depicts the sequential flipping process (overall barrier

(42) These fragments originate from the bent and linear metallocenes JEDPEN and SUHLEM, respectively.

(43) Dynamic NMR data for this interconversion process have only been reported for the crowded derivatives $[(C_6F_5)_4C_5H]M(CO)_3$ (M = Mn or Re); in either case, the *β* C_6F_5 moieties are in slow exo(distal)−endo(proximal) exchange at all temperatures in the ^{19}F regime, whereas rotation of the α ring is not frozen out until 198 K, yielding $\Delta G^{\ddagger}$ values of 8.0 ± 0.2 kcal mol^{-1}. See: Thornberry, M. P.; Slebodnick, C.; Deck, P. A.; Fronczek, F. R. *Organometallics* **2001**, *20*, 920−926.

(44) Alvarez-Toledano, C.; Baldovino, O.; Espinoza, G.; Toscano, R. A.; Gutiérrez-Pérez, R.; García-Mellado, O. *J. Organomet. Chem.* **1997**, *540*, 41−49.

(45) Evrard, P. G.; Piret, P.; Germain, G.; van Meerssche, M. *Acta Crystallogr.* **1971**, *B27*, 661−666.

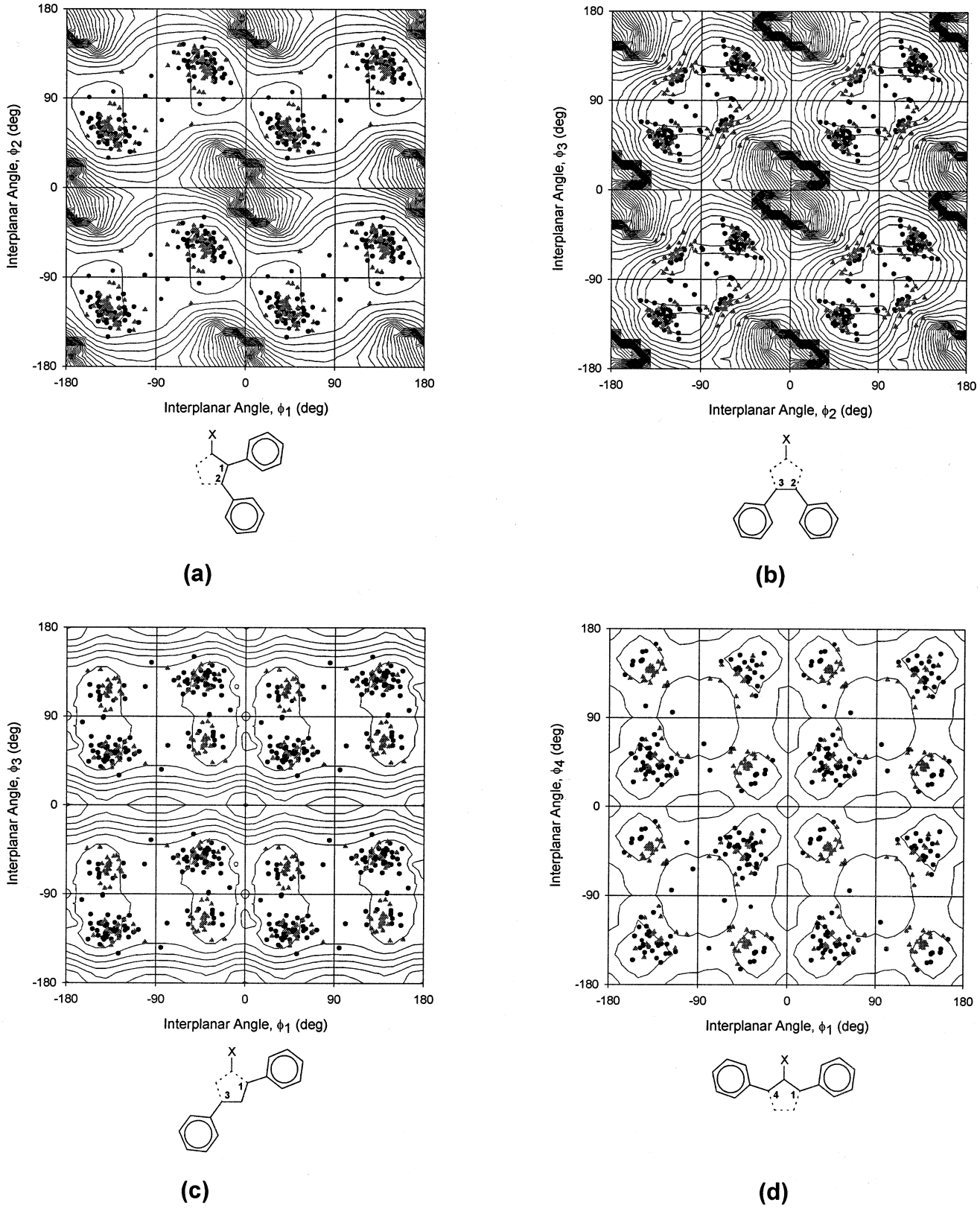

FIGURE 4. Conformational maps of torsional angles of two peripheral aryl rings constituting part of a Ar_4C_4CX frame (X ≠ Ar; *C*-X = sp^2 (triangles) and sp^3 (circles) hybridized), featuring vicinal (a) (1,2/4,3) and (b) (2,3), as well as next-nearest (c) (1,3) and (d) (1,4) interactions. The overlayed contours (at 1.5 kcal mol^{-1}) represent the calculated (AM1) equipotential energy regions associated with $C_4Ph_4C{=}O$ (**3**).

of 1.7 kcal mol^{-1}), symmetrically disposed about the transition state **1**-TS2 in which one of two adjacent aryl groups has completely reversed helicity and the buttressing phenyl substituents are approaching orthogonality. The rearrangement of **2**-C_2 ⇌ **2**-C_2' also constitutes three steps (Schemes 2b and 3b), with a slightly steeper energy

SCHEME 2. Intermediate and Transition Structures (AM1 Hamiltonian) Involved in Flipping Processes (a) 1-D_5 ⇌ 1-D_5' and (b) 2-C_2 ⇌ 2-C_2' As Viewed along the 5-Fold or Perpendicular to the 2-Fold Symmetry Axes in 1-D_{5h} and 2-C_{2v}, Respectively[a]

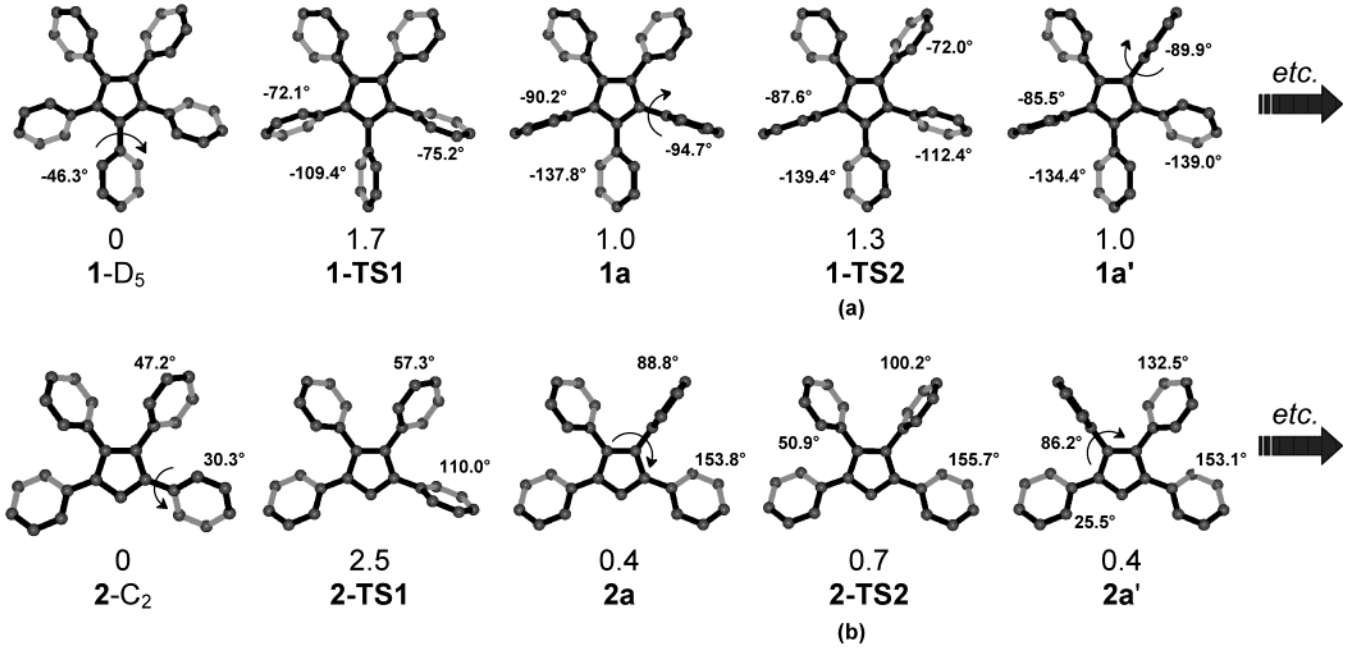

[a] The dihedral angles (∠ = $C_5(\alpha)-C_5(ipso)-C_6(ipso)-C_6(\alpha)$) are measured counterclockwise around the C_5 ring. The relative energies are given in kcal mol^{-1}.

profile and a barrier height of 2.5 kcal mol^{-1}. The corresponding inversion of configuration of propellers **3** and **4** has not been completely characterized, but by analogy, the relative energies of the first transition structures (**3**-TS1, **4**-TS1), wherein an α ring has rotated beyond its perpendicular orientation, are 1.6 and 1.0 kcal mol^{-1}, respectively. Particularly noteworthy is the agreement of the calculated angles in the various saddle points with the crystallographic orientations of the peripheral blades along the gearing trajectories evinced in the two-dimensional conformational maps. In all four molecules, concerted *n*-ring (see **1**-D_{5h}, **2**-C_{2v}, **3**-C_{2v}, **4**-C_{2v}) and (*n*−1)-ring flip mechanisms are easily discounted given the number of imaginary vibrational frequencies associated with the relevant stationary points. So while the earlier suppositions of Pepermans et al.[8a] are confirmed herein, we have also extended the model beyond the permutational sense, which is devoid of all mechanistic details.

There is one final corollary that should not be overlooked. According to the parity restriction on dynamic gearing, uncorrelated as well as correlated rotation is mechanically disallowed in a closed cyclic array consisting of an odd number of securely meshed gears, thus inducing immobility.[46] While the operation of this rule has precedent in triptycyl-based molecules,[15,47] propeller frameworks composed of aryl rings (2-fold rotors) may not present the obligatory "tongue and groove interactions" for such interdependent rotation, allowing for *gear slippage* in the dynamic regime.[48] Furthermore, the efficient transmission of information via cooperative torsional motions along a macromolecular chain of coupled rotors is limited not only by the extent of steric interplay but by the length of the propeller chain and the inversely related energy gap between uncorrelated and correlated rotational pathways.[9a,49] By deductive reasoning C_5Ar_5-systems are exempt from the strict specificity of cogwheeling and therefore exhibit a preference for successive localized (con/dis)rotations of adjacent rings over concerted ring-flip mechanisms. Alas, there is no disparity in the parity principle!

Conclusions

Analysis of C_5Ar_5 and C_5Ar_4X moieties by the structure correlation method indicates an equilibrium propeller orientation, although species belonging to the latter class exhibit increased conformational flexibility by virtue of different α and β steric environments. On the basis of the qualitative agreement between the AM1 calculated potential energy surfaces and the experimental distribution of data points generated from the diaryl (C_{2v} and C_s symmetric) models, an extended torsional itinerary corresponding to an entropically favored nonsynchronous (i.e., delayed) *n*-ring flip has been constructed for all tetra- and pentacycles. Without an index of comparison (i.e., empirical data) to evaluate the quality of our computations or our description of this stereoisomerization process, we can only submit that the highly organized transition states associated with a concerted mechanism are much less probable. The observation of helicity reversal by use of dynamic NMR methods requires the incorporation of diastereotopic probes, such as pendant *p*-$CH^{19}F_2$ groups on the peripheral aryl rings, that are

(46) Mislow, K. *Chemtracts: Org. Chem.* **1989**, *2*, 151−174.
(47) Chance, J. M.; Geiger, J. H.; Mislow, K. *J. Am. Chem. Soc.* **1989**, *111*, 2326−2327.
(48) Among the numerous examples of statically geared systems, hexaisopropylbenzene is probably the most spectacular. See: (a) Arnett, E. M.; Bollinger, J. M. *J. Am. Chem. Soc.* **1964**, *86*, 4729−4731. (b) Siegel, J.; Gutiérrez, A.; Schweizer, W. B.; Ermer, O.; Mislow, K. *J. Am. Chem. Soc.* **1986**, *108*, 1569−1575. (c) Biali, S. E.; Gutiérrez, A.; Mislow, K. *J. Org. Chem.* **1988**, *53*, 1316−1318.
(49) Bettinger, H. F.; Schelyer, P. v. R.; Schaeffer, H. F. I. *J. Am. Chem. Soc.* **1998**, *120*, 1074−1075.

SCHEME 3. Graphical Representation of Potential Energy Surfaces Associated with Correlated Inversion of the Propeller Forms of (a) 1 and (b) 2

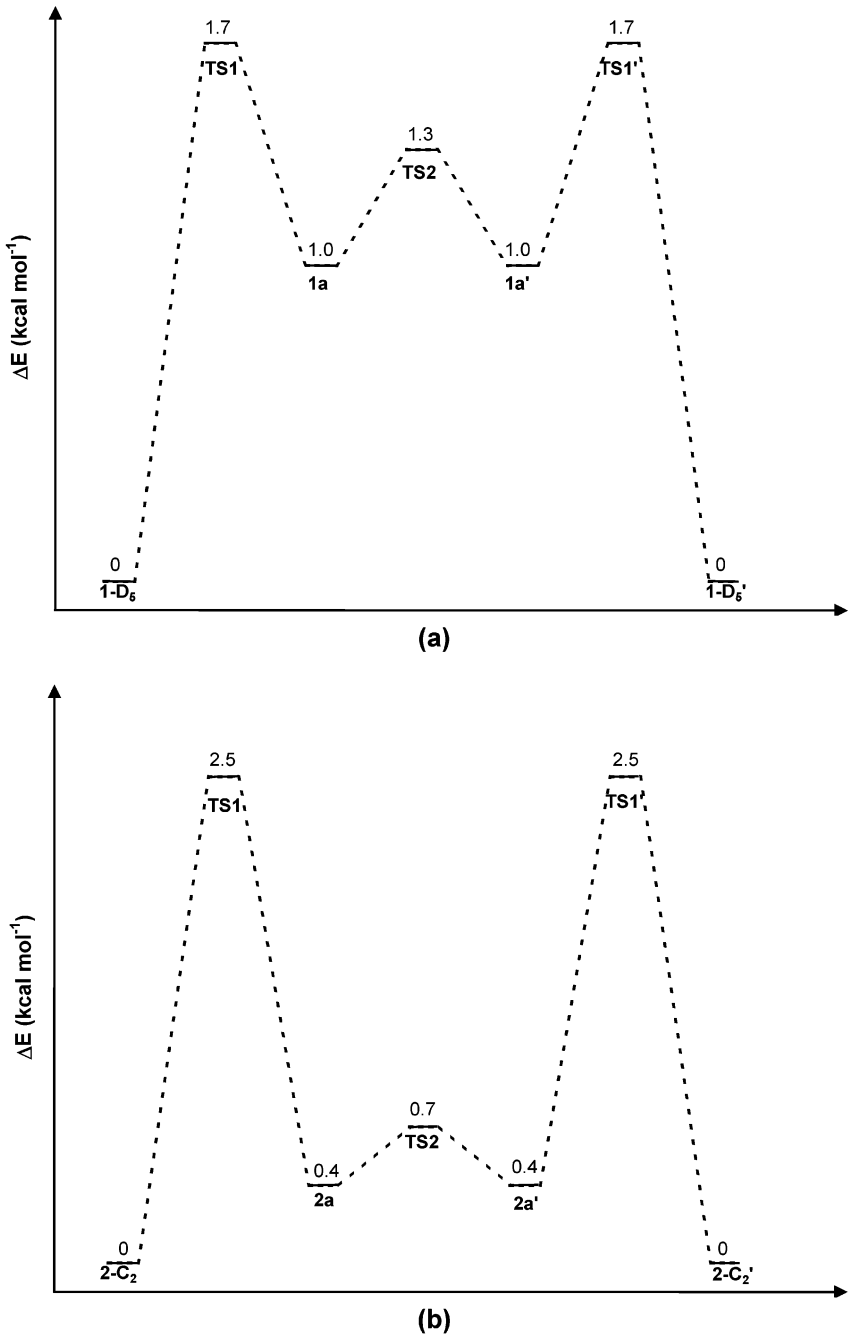

rendered enantiotopic (and therefore necessarily isochronous in an achiral solvent) in a symmetrized environment. In the absence of increased repulsive nonbonded interactions of the flipping rings (such as mesityl or 2,6-xylyl substituents), however, the calculated rotational barriers are well below the range accessible by such techniques. In an endeavor to transcend the timescale limitations of NMR spectroscopy, the challenge remains for experimentalists to devise variable-temperature EPR studies that might further probe the generality of this correlated inversion process in propeller systems comprised of a central planar, polyatomic framework.

Acknowledgment. This research was supported by the Natural Sciences and Engineering Research Council of Canada (NSERC). S.B. gratefully acknowledges both the Government of Ontario and NSERC for graduate scholarships. We also extend our profound appreciation to a reviewer for his/her insightful, conscientious, and encouraging comments.

Supporting Information Available: Supplementary CSD data for C_5Ar_5, C_4Ar_4CX, and $C_4Ar_4CX_2$ fragments. Conformational maps with calculated (MMFF94) torsional potential energy surfaces associated with $C_5Ph_5^-$ (**1**), $C_5Ph_4H^-$ (**2**), and $C_4Ph_4C{=}O$ (**3**). Cartesian coordinates, total energies, and lowest vibrational frequencies of all AM1 optimized geometries (**1**−**4**). This material is available free of charge via the Internet at http://pubs.acs.org.

JO0201272